JOURNAL OF PROPULSION AND POWER
Vol. 10, No. 4, July–Aug. 1994

Nonequilibrium Combustion Model for Fuel-Rich Gas Generators

Robert O. Foelsche,* Joseph M. Keen,* and Wayne C. Solomon†
University of Illinois, Urbana, Illinois 61801
and
Parker L. Buckley‡ and Edwin Corporan§
Wright-Patterson Air Force Base, Ohio 45433

The efflux composition characteristics of an experimental fuel-rich gas generator have been modeled with a detailed hydrocarbon kinetics package that includes the effects of liquid droplet vaporization. The chemical reaction mechanism, consisting of 107 chemical species and 642 reversible reactions, is capable of describing a complex kerosene-type fuel mixture for the case where the constituents (aliphatic, aromatic content) can be specified. A liquid fuel droplet vaporization model for octane and toluene mixtures has been included. A flame zone model is incorporated to address the fast reaction phenomena necessary for sustained combustion. Successful modeling has necessitated the use of a nonequilibrium approach incorporating a detailed chemical model. Comparison of modeling results to experimental data has shown good agreement, clearly supporting nonequilibrium operation.

Nomenclature

A_i = Arrhenius preexponential factor
B = Spalding transfer number
C_xH_y = nomenclature for chemical compounds
c^* = characteristic exhaust velocity
c_{pk} = gas phase specific heat, cal/g/K
d_0 = nominal initial droplet diameter, cm
E_i = activation energy, Kcal/mol
h_k = specific enthalpy per unit mass
j = stoichiometric fuel-oxidant mass ratio
k_{fi} = forward rate constant of ith reaction
k_{ri} = reverse rate constant of ith reaction
L = latent heat of vaporization, cal/g
MR = mixture ratio
$\dot{m}$ = mass flow rate through reactor, g/s
P_c = reactor chamber pressure, atm
Q = reactor heat loss
q_i = rate of progress variable
q^0 = heat of reaction, cal/g
R_c = universal gas constant
T_c = reactor chamber temperature, K
T_L = temperature at the droplet surface, K
T_{RXN} = flame zone kinetic temperature, K
V = reactor volume, cm^3
W_k = molecular weight of species k
Y_k = mass fraction
$Y_{0,\infty}$ = oxidizer mass fraction at infinity
β_i = non-Arrhenius temperature exponent
λ = gas phase thermal conductivity
ν'_{ki} = stoichiometric coefficients of the reactants
ν''_{ki} = stoichiometric coefficients of the products
ρ = mixture density, g/cm^3
ρ_l = droplet liquid density, g/cm^3
τ = reactor residence time, ms
τ_l = nominal droplet lifetime, ms
Φ = equivalence ratio
$\dot{\omega}_k$ = molar production rate per unit volume

Introduction

THE requirement for advanced propulsion systems operating in the Mach 0.5 to Mach 6 flight regime has been identified as a major focus for future flight missions. For many of these applications, air-breathing systems are desirable from the aspect that the oxidizer need not be carried along as system weight. The current state of the art in air-breathing technology limits the operating speeds to the Mach 3+ range. Thus, there is a need for new technology to bridge the gap in the flight speed envelope.

One of the more promising concepts in the advanced propulsion effort is the ramrocket or rocket ramjet. In this design, a solid- or liquid-fueled rocket is employed in the role of a gas generator to create a fuel-rich effluent for subsequent combustion with oxidizer entrained from the freestream air. By harnessing the additional potential of the partially combusted efflux, these two-stage devices can realize significant gains in performance over rocket propulsion elements. The somewhat higher complexity resulting from the air-breathing design, as compared to a pure rocket, is outweighed by the increased range that is achieved.

Of major concern in such a design is the performance of the gas generation system under varying operating conditions. In particular, it is important for the propulsion systems designer to know the composition and condition of the effluent prior to the ducted combustion section. This is critical to determining the extent of the benefit that may be derived from the two-stage design. In an effort to extend the technology base of fuel-rich gas generators, an experimental simulation of a solid-fueled gas generator is currently underway.[1,2] This effort coupled with previous work on kinetically dominated gas generation sources is being used to investigate fuel efflux characteristics and production techniques. The work is being conducted to gain a better understanding of the pa-

Presented as Paper 93-2041 at the AIAA/SAE/ASME/ASEE 29th Joint Propulsion Conference and Exhibit, Monterey, CA, June 28–30, 1993; received July 8, 1993; revision received Dec. 30, 1993; accepted for publication Jan. 11, 1994.

*Graduate Research Assistant, Department of Aeronautical and Astronautical Engineering. Student Member AIAA.
†Professor and Department Head, Department of Aeronautical and Astronautical Engineering. Associate Fellow AIAA.
‡Lead Engineer, Aeropropulsion and Power Directorate. Senior Member AIAA.
§Engineer, Aeropropulsion and Power Directorate.

rameters that influence the fuel gas composition and to document expected fuel-rich compositions.

In addition to experimental work, an effort in computational modeling has been undertaken to make available predictive capabilities.[3,4] Previous experimental work performed in conjunction with numerical simulation has indicated that fuel-rich gas generation devices do not achieve chemical equilibrium within the residence times afforded by the hardware.[1,4-7] Heubner[6] has documented c^*, combustion temperature, and efflux compositions for various mixture ratios of methane and RP-1 propellant in a gas generator application. Equilibrium predictions compared to the data indicate consistent overprediction of c^* and solid carbon content with generally poor agreement between the data and modeling predictions. In early investigations, Lawver[7] conducted an experimental and modeling study on large, high-pressure preburners fueled by RP-1. Efflux compositions and c^* were shown to be inadequately modeled by an equilibrium formulation. A nonequilibrium formulation employing a semiglobal fuel decomposition description with empirically fitted rates for the preliminary steps was shown to result in improved predictive capabilities over the range of operating conditions studied.

Desaulty and Chauveau[5] have demonstrated the ability of a perfectly stirred reactor formulation coupled with a detailed nonequilibrium chemical reaction mechanism to accurately model properties in the combustor unit of a gas turbine engine. Evaluating three levels of nonequilibrium chemical modeling, they concluded decisively through comparative results that a more detailed-step, kinetic model outperformed in all respects global or semiglobal decomposition schemes. More recently, Buckley[1] and Corporan[2] have obtained detailed experimental efflux characterizations for ethylene/toluene- and JP-7/toluene-fueled gas generator efflux simulators which have shown the devices to operate nonequilibrium. Due to the poor predictive capabilities of the available equilibrium modeling codes, an effort was undertaken to produce a flexible nonequilibrium model for use with high-pressure, fuel-rich hydrocarbon systems.

Since chemical kinetic limits were suspected to be the major cause for the overall nonequilibrium operation, a detailed chemical reaction approach was employed. Such an approach requires considerable computational expenditure toward solving the chemistry, let alone the fluid dynamics of the flow. In order to preclude excessive computing requirements inherent in three-dimensional reacting flow algorithms solving the full set of flow equations, a simpler technique was demanded. The model selected was a perfectly stirred reactor (PSR) formulation. Based on experimental observations[1] and previous successes with such an approach,[5] this model was deemed appropriate for the present application despite the inherent deficiency of the formulation in composing the convective and diffusive fluxes. Our model is based on a formulation similar to that employed successfully by Desaulty and Chauveau.[5] In addition, considerations for liquid spray vaporization (Spalding model) and a flame zone model (two-temperature approach) describing the fast reaction, high-temperature zone that exists in the injector region have been included.

In addition to the availability of a robust and efficient fluid dynamic simulation, an accurate kinetic mechanism describing the decomposition and oxidation of the fuels of interest is of primary importance to the modeling study. An acceptable reaction scheme in the level of detail demanded was not available in the literature, hence, it was necessary to construct one. A hydrocarbon mechanism capable of modeling aliphatic species up to C8-alkane molecules plus the aromatics of toluene, benzene, and related intermediates has been formulated. Through combinations of the modelable fuels included in the proposed set, it is possible to model hydrocarbon mixtures for cases where the individual constituents of the mix, both aliphatic and aromatic, can be specified. Validation of the completed scheme against numerous independent combustion data has demonstrated the integrity of our final mechanism.[3]

Numerical Model

In the perfectly stirred reactor formulation it is assumed that mixing is infinitely fast and that properties are uniform throughout. Hence, both spatial- and time-dependent characteristics of the fluid dynamic process are absent. The mass and energy equations are satisfied with appropriate consideration for the species source terms generated through the combustion process. Under the simplifying assumptions of the stirred reactor model, the fluid dynamic equations take the following form:

species conservation

$$\dot{m}(Y_k - Y_k^*) - \dot{\omega}_k W_k V = 0 \tag{1}$$

conservation of energy

$$\dot{m} \sum_{k=1}^{K} (Y_k h_k - Y_k^* h_k^*) + Q = 0 \tag{2}$$

where inlet conditions are indicated by the superscript (*).

Although the equations as posed above are indeed invariant in time, the numerical algorithm utilized may require the solution of the related time-dependent problem to obtain convergence. The equations for the transient problem are then

$$\rho V \frac{dY_k}{dt} = -\dot{m}(Y_k - Y_k^*) + \dot{\omega}_k W_k V \tag{3}$$

$$\rho V \frac{dh}{dt} = -\dot{m} \sum_{k=1}^{K} (Y_k h_k - Y_k^* h_k^*) - Q \tag{4}$$

The time-invariant equations form a set of $K + 1$ nonlinear algebraic equations, whereas the transient equations compose a $K + 1$ deg nonlinear ordinary differential equation initial value problem. This formulation[8] is convenient in that it allows the use of a single solution technique for both problems.

The chemical source terms $\dot{\omega}_k$ represent the net rate of production of each individual species. This rate can be expressed as a summation of the individual progress terms for each reaction. Considering a set of reactions of the form

$$\sum_{k=1}^{K} \nu'_{ki} \chi_k \rightleftharpoons \sum_{k=1}^{K} \nu''_{ki} \chi_k \tag{5}$$

the term $\dot{\omega}_k$ can be written

$$\dot{\omega}_k = \sum_{i=1}^{I} \nu_{ki} q_i \tag{6}$$

where

$$\nu_{ki} = (\nu''_{ki} - \nu'_{ki}) \tag{7}$$

and the rate of progress variable is given by

$$q_i = k_{fi} \prod_{k=1}^{K} (\chi_k)^{\nu'_{ki}} - k_{ri} \prod_{k=1}^{K} (\chi_k)^{\nu''_{ki}} \tag{8}$$

In this formulation the k_{fi} are given by the modified Arrhenius representation

$$k_{fi} = A_i T^{\beta_i} \exp(-E_i/R_c T) \tag{9}$$

whereas the reverse rates are calculated through the equilibrium constant determined from the thermodynamic properties of the species involved.

A baseline stirred reactor code made available for the present investigation was developed by Glarborg et al.[8] The system of equations is solved using a damped, modified Newton algorithm. This is an iterative approach which constructs a series of approximate solution vectors to the set of governing equations. In general, the nth such iterate will not identically solve the governing equations, but will give a residual vector $\boldsymbol{F}$ containing the variation in the solution. The objective is to determine a solution vector $\boldsymbol{\phi}$ such that

$$\boldsymbol{F}(\boldsymbol{\phi}) = 0 \tag{10}$$

For the PSR code, $\boldsymbol{\phi}$ is the vector of temperature and species mass fractions

$$\boldsymbol{\phi} = (T, Y_1, \ldots, Y_k, \ldots, Y_K)^T \tag{11}$$

and $\boldsymbol{F}$ contains the energy and species continuity equation residuals.

The original stirred reactor formulation considered prevaporized, premixed combustion without regard to the propellant injection and vaporization issues or ignition processes. The latter are known to be important for our case. In order to produce the gas generator model, modifications have been made to incorporate these issues within the limitations imposed by the perfectly stirred reactor idealization while maintaining the fairly modest computational requirements.[4] The droplet model selected is an implementation of the classic Spalding model considering the combustion of a single fuel droplet of specified diameter in a quiescent oxidizing atmosphere.[9] While we acknowledge that convective and size ensemble effects (among others) will be important for problems such as those under consideration, the primary goal of the present investigation is not to create a detailed liquid stream vaporization formulation, but rather to identify the relative importance of the various phenomena present within the chamber. In the results, it is shown that the droplet vaporization/combustion process is of secondary importance compared to the chemistry (as are the fluid dynamic effects as hypothesized). To this end, the model is adequate to impose the character of the evaporative process without strictly defining the nature of the phenomenon and unnecessarily increasing the complexity of the calculations. This allows the inclusion of an additional parameter in the form of an effective droplet diameter which may be examined for "net" influence of vaporization time.

Since the Spalding analysis is presented in many sources (e.g., Ref. 4), we will only present the pertinent results here as they apply to our problem. Applying the Spalding assumptions to the governing equations, a droplet lifetime can be shown to be given by

$$\tau_l = [c_p \rho_l d_0^2 / 8\lambda \ln(1 + B)] \tag{12}$$

where B is defined as

$$B = (1/L)[c_p(T_\infty - T_L) + (q^0 Y_{0,\infty}/j)] \tag{13}$$

The fuel properties in B and τ_l are calculated from empirical correlations.

Droplet vaporization affects the PSR computation in two ways. First, there is a reactor heat loss due to the enthalpy addition required to evaporate the fuel droplet. Secondly, the reactor combustion time is modified to account for the finite time required in vaporizing the droplet. These effects are calculated for each of the liquid propellants specified.

The evaporative heat loss term is a straightforward modification for a given fuel type. The initial fuel enthalpies in the conservation equations employ the values for the liquid fuel at the inlet temperature. The heat required to raise the droplet to the boiling point temperature as well as the latent heat utilized in the gasification of the fuel are accounted for through the difference between the gaseous and liquid phase enthalpies.

The residence time available for combustion is calculated from the total residence time by decreasing the total time by the greatest mean lifetime of a fuel droplet. The maximum computed lifetime for any of the droplet species is subtracted from the input reactor residence time (or calculated in the case of an input mass flow rate); i.e.,

$$\tau = \tau_0 - \tau_l^* \tag{14}$$

where the superscript (*) indicates the maximum value. This approach gives a lower limit for combustion time. In actuality, combustion of the vaporized portion of the fuel could proceed prior to complete evaporation, so that our approximation will only hold if the vaporization times are small compared to the total reactor residence time. Factors other than those mentioned that tend to increase the vaporization rate have been neglected.

To model the combustion process, a two-temperature model for the reactor has been selected.[4] This has been found to provide an improved idealization of the actual combustion process. A temperature more consistent with the actual combustion of injected liquid fuel droplets is used to drive the kinetics, effectively decoupling the fluid dynamic and chemical processes. This kinetic temperature modification is necessary to "start" the reactor with the proper enthalpy values consistent with a hot flame zone near the injector region. This second temperature (T_{RXN}) is more representative of the stoichiometry in the injector region flame zone than the final bulk temperature that is commonly measured at points far removed from the injector. The bulk T_c obtained using the present approach are in good agreement with the available results.

The effect of this procedure on gas composition is also important. Since the concept is applied throughout the combustion sequence, it is necessary to employ a kinetic temperature T_{RXN} in the range indicated in the experimental section. Failure to do so leads to erroneous results: at temperatures too high, artificial cracking of the uncombusted fuels and higher order intermediates occur; at temperatures significantly lower one finds incomplete combustion. Temperatures outside this narrow range are not supported by experimental data.

Kinetics

At the operating temperatures resulting in our fuel-rich hydrocarbon reactor, combustion is dominated by the nonequilibrium processes. Numerous species have been identified as important intermediates to the fuel mixture decomposition, thus requiring the construction of a large reaction set. With the purpose of modeling the controlling combustion processes in detail, a hydrocarbon combustion mechanism has been developed to describe the pyrolysis and oxidation steps for the complex hydrocarbon fuel mixture. This detailed, elementary-step reaction mechanism considers hydrocarbons up to the C8-alkane species n-octane and the aromatics toluene and benzene, plus their important intermediate species. The mechanism describes in detail the breakdown of fuel molecules through numerous intermediates species into final products. The set includes a modification of the soot formation scheme developed by Nickerson and Johnson for gas generators.[10]

It was necessary to construct this set from individual mechanistic studies since no single mechanism covering the range of hydrocarbons of interest was available in the literature. The chemical reaction mechanism, consisting of 107 chemical species and 642 reversible reactions, is capable of describing the studied complex fuel mixture. Earlier work with a smaller

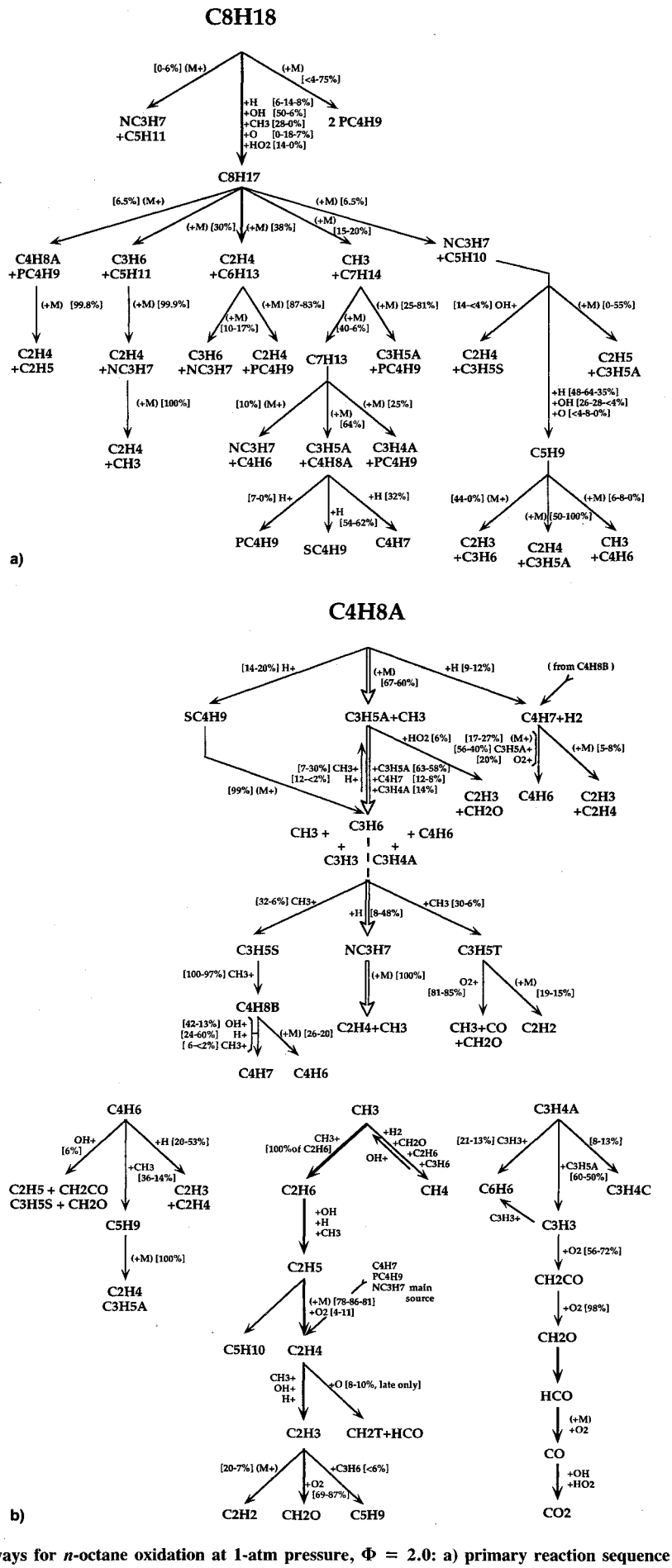

Fig. 1 Decomposition pathways for *n*-octane oxidation at 1-atm pressure, $\Phi = 2.0$: a) primary reaction sequence and b) pathways for the 1-butene and lower hydrocarbons.

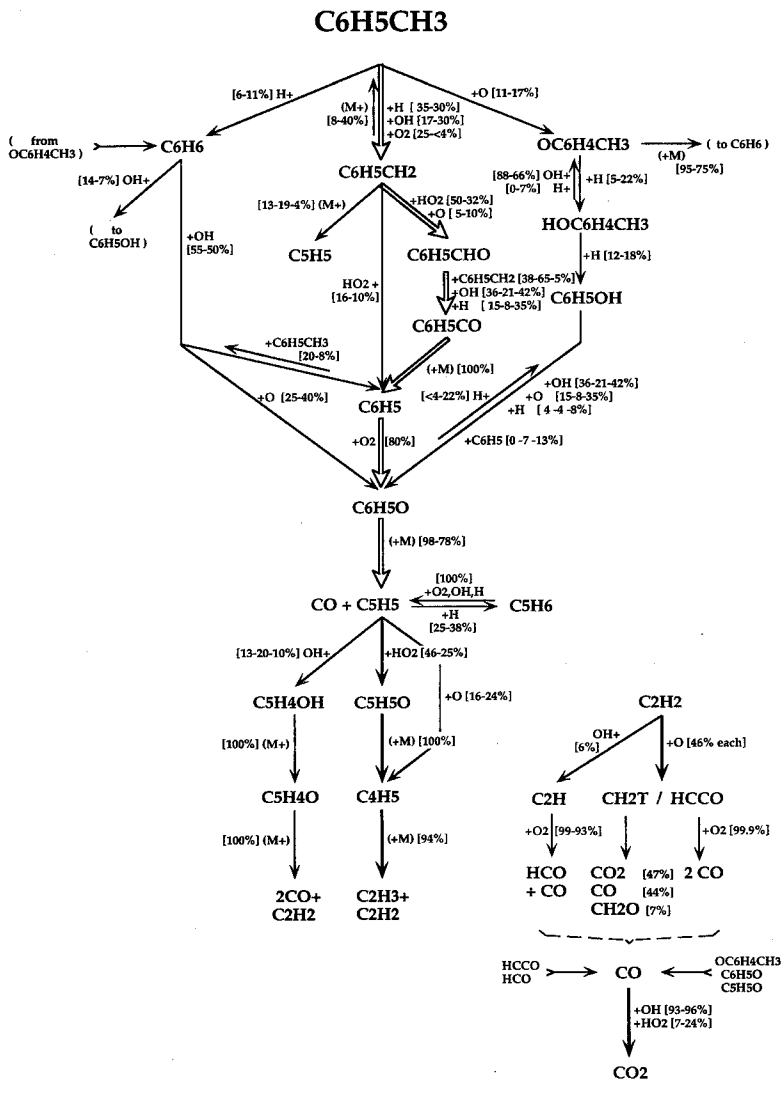

Fig. 2 Decomposition pathways for toluene oxidation at 1-atm pressure and fuel lean conditions (Φ = 0.69).

set of chemical reactions was less satisfactory at fuel rich conditions.[3] Unfortunately, due to space limitations this mechanism could not be reproduced here. The full reaction set and the details of its construction, accompanied by extensive validation of the important submechanism to various data, can be found in Ref. 3. The final mechanism can be obtained in report format or electronically from the authors.[11] The proposed kinetic scheme can in addition to *n*-octane and toluene describe the decomposition of the species methane, ethylene, ethane, propene, propane, 1-butene, *n*-heptane, and benzene.

Since JP-7 is in itself a mixture of aliphatic chain species and aromatics, we chose to represent it by an equivalent mixture of *n*-octane (representative in properties of the aliphatic in JP-7) and toluene (an aromatic representative of those in kerosene as well as an additive in the current combustion study). These two species comprise the equivalent fuel mixture which was used to computationally investigate the combustion properties of the gas generator fuel mixture. Modeling has shown the equilibrium product distributions to agree closely for the JP-7 and *n*-octane/toluene-mix fuel formulations.[4] Typical decomposition characteristics for *n*-octane and toluene will now be described.

The arrows in the following figures indicate the progression of hydrocarbon fuel molecule decomposition into products along the elementary reaction steps, where the reaction partners are listed alongside the arrows. The numbers in brackets correspond to the contribution of reactive decomposition flux by the listed reaction partner for the selected conditions of the corresponding experimental data. Where several numbers appear it is meant to indicate a range of decomposition flux as reaction progresses (either in time or in temperature). These percentages were obtained by investigating the individual contributions to each species' decomposition by the respective partner, a quantity given by a normalization of the terms $C_{ki} = \nu_{ki} q_{ki}$ in the sum forming $\dot{\omega}_k$ in Eq. (6).

n-Octane Oxidation Chemistry

Normal octane is presently the largest chain molecule which can be described by the detailed mechanism. There are few detailed modeling studies of the large aliphatic species which include experimentally determined rate constants or verified product routes. Insufficient basic research regarding measurement of elementary rate constants and identification of competing product routes has necessitated the use of several approximations in the fuel decomposition formulation. Many of the reaction mechanisms in the literature and the corresponding rate parameters have been estimated from analogous reactions in related fuels. However, Warnatz[12] has shown that fuel removal steps for the larger aliphatic hydrocarbons are similar to those found within the butane submechanism, and this observation has greatly assisted the construction of the higher hydrocarbon mechanisms. The kinetics for the present *n*-octane decomposition description were taken primarily from the works of Westbrook and Pitz[13] and Chakir et al.[14] Considerable review of the C4 and lower species submechanisms was conducted as well.[3]

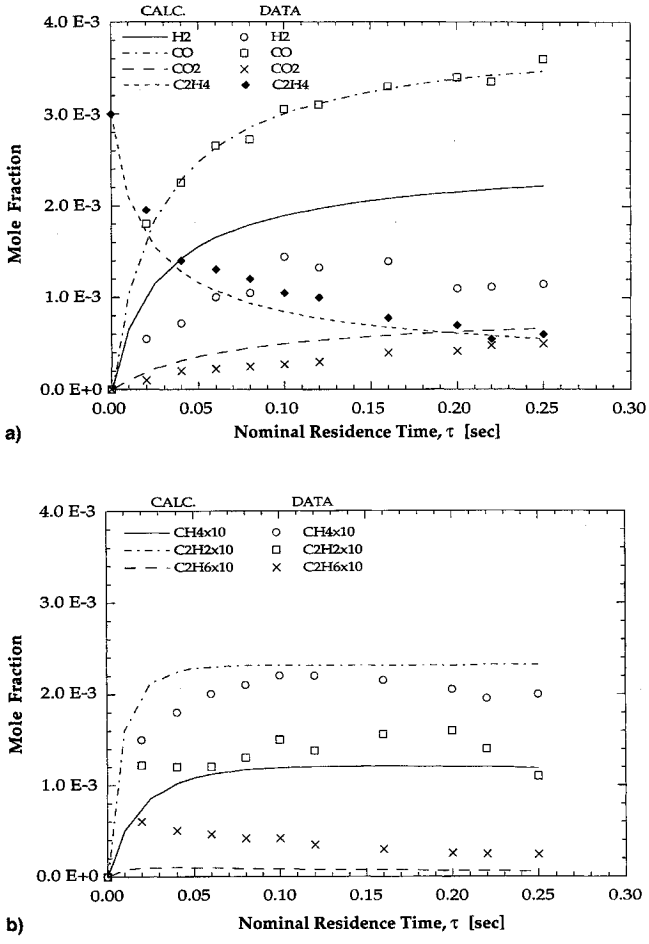

Fig. 3 Fuel rich ethylene oxidation in perfectly stirred reactor at 1 atm, Φ = 2.0, with initial temperature 1163 K: a) major species and b) minor intermediates. Lines are calculated values, symbols represent data. Data from Dagaut et al.[18]

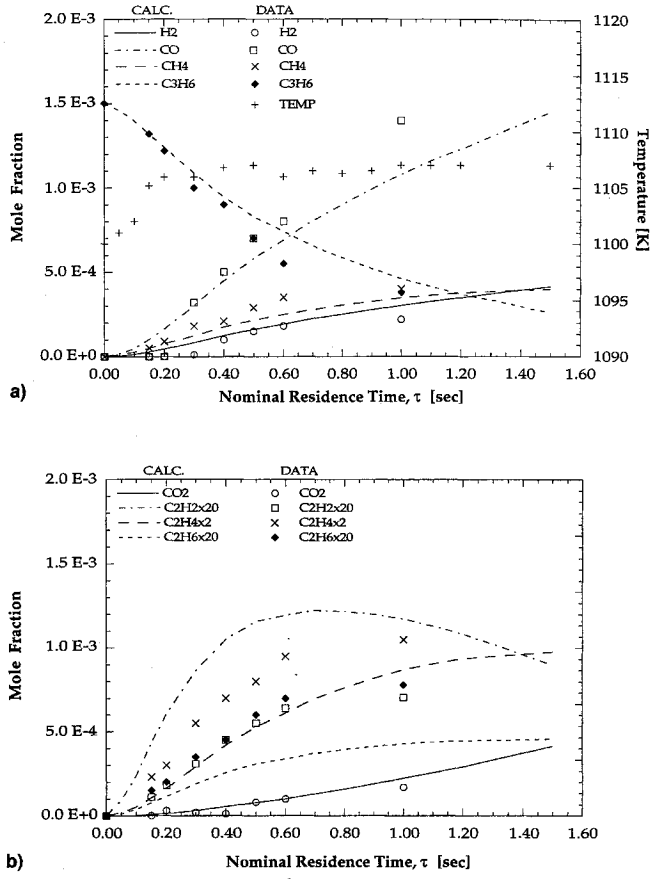

Fig. 4 Species concentrations for propene oxidation in perfectly stirred reactor at 5 atm, Φ = 1.0, with initial temperature 1100 K: a) major species and b) minor intermediates. Data from Dagaut et al.[19]

Typical *n*-octane decomposition and oxidation at fuel-rich conditions (Φ = 2.0, 1 atmosphere pressure, temperature range 930–1240 K) is shown in Figs. 1 and 1b. The parent fuel molecule is seen to decompose by thermal pyrolysis reactions leading to primary butyl radicals (pC_4H_9), or by hydrogen atom abstractions to produce the octyl radical (C_8H_{17}). Butyl radicals decompose further by C—C bond scission at most combustion conditions. This process is the primary source of ethylene, an important intermediary hydrocarbon. The octyl radical also decomposes through C—C bond scission leading to the following intermediates listed in order of importance to decomposition flux under these prescribed conditions: pentyl radical (C_5H_{11}), hexyl radical (C_6H_{13}), 1-heptene (C_7H_{14}), pentane (C_5H_{10}) and the products, butyl radical (pC_4H_9) and 1-butene (C_4H_8A).

Oxidation does not play a significant role in the initial stages of fuel molecule decomposition. The primary reaction sequence is through pyrolysis or hydrogen atom abstraction followed by pyrolysis. Decomposition of the C4 species typically proceeds as shown in Fig. 1b. Through a series of thermal decomposition steps and radical-radical reactions, the C4 species C_4H_8A and pC_4H_9 decompose down through C3 species including propene, allene, and propyl radical into the C2 and lower species. The primary intermediates are ethylene, acetylene, and methyl radical (which accounts for the methane present). Further decomposition of these C2 and lower species is primarily via oxidation steps. The oxidation steps include ethylene to form formaldehyde CH_2O, and formyl radical HCO, which then lead directly to the combustion products CO and CO_2. These steps are responsible for the heat release and conversion of intermediates into final products. Only when the C2 hydrocarbon level is reached does direct oxidation begin to play the major role.

Reaction maps such as those in Figs. 1a and 1b, and the analogous map for toluene, display the interrelation of various species and their role in the decomposition process. Such figures were constructed for all the important submechanisms considered to provide insight into the combustion modeling while providing a basis for comparison to the works of other researchers. It is noted that oxidation occurs relatively late in the overall fuel molecule decomposition scheme for the aliphatic constituents. This indicates that these species in the fuel mixture will decompose readily even at low temperatures and oxygen-lean conditions such as those of our gas generator application. This is in stark contrast to the decomposition behavior of the aromatics detailed next.

Toluene Oxidation Chemistry

Toluene comprises the major portion of the fuel mixture employed in our experimental gas generator as well as in our simulated mixture. An accurate representation of the decomposition and oxidation sequence for this species is thus vital to the present modeling study. Toluene oxidation has received extensive experimental and modeling attention only in the past several years; the chemistry is likely the least well known of the reaction sets included, except over a narrow range of operating conditions. The chemical reaction mechanism employed for toluene was taken primarily from the mechanistic modeling work of Emdee et al.,[15] which is in turn based on the modeling and experimental work of Brezinsky.[16] Their results were produced from studies at temperatures near those of interest to the present application.

Figure 2 presents a schematic reaction map for typical toluene decomposition at fuel lean conditions (Φ = 0.69, 1 atm, average temperature of 1190 K) corresponding to experimental data given in Ref. 15. Decomposition proceeds pri-

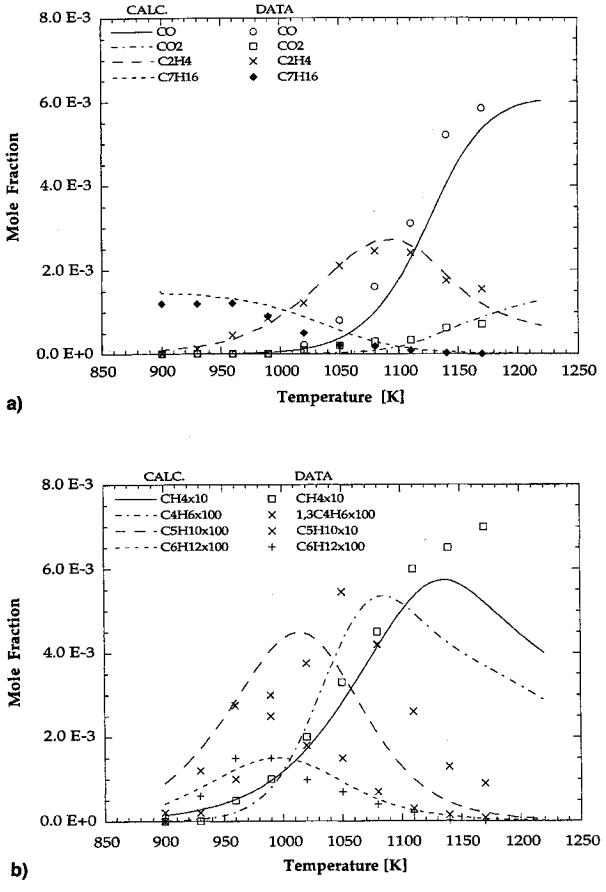

Fig. 5 Species concentrations for *n*-heptane oxidation in perfectly stirred reactor at 1 atm, $\Phi = 2.0$, and $\tau = 0.2$ s: a) major species and b) minor intermediates. Experimental data from Chakir et al.[14]

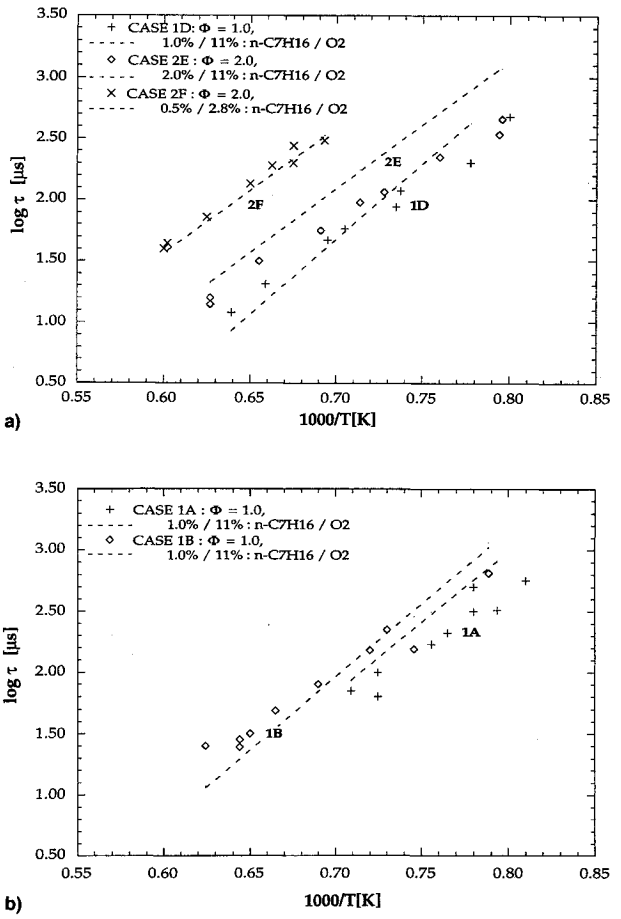

Fig. 6 Ignition delay times for *n*-heptane behind reflected shock wave: a) at $\Phi = 1.0$, 2.0, 2.0 and b) both at $\Phi = 1.0$, various pressures. Data from Burcat et al.[20]

marily through the intermediate benzyl radical ($C_6H_5CH_2$) and benzene (C_6H_6), both of which further break down through various mechanisms to produce the phenyl radical (C_6H_5) and phenoxy radical (C_6H_5O). This initial reaction sequence is characteristic of the lower temperature ranges ($T < 1500$ K) where oxidation is the primary course as opposed to the thermal cracking observed at higher temperatures. Since our gas generator temperatures are typically limited to maximums on the order of 1600 K corresponding to the values in the injector region flame zone, oxidation is the only major decomposition route available in this fuel-rich environment.

The subsequent ring opening sequence of reactions proceeds exclusively by thermal decomposition, even at these low temperatures, through the phenoxy radical and then the cyclopentadienyl radical (C_5H_5). The latter species further decomposes through oxidation reactions leading to the C4 and acetylene subspecies that then either oxidize or contribute to soot formation.

The significant difference between the decomposition of the aliphatic and aromatic constituents is the character of the initial fuel molecule decomposition and the role which oxygen species play. Species containing oxygen are critical to toluene and benzene but are less important for primary *n*-octane decomposition. Distinct characteristics of the fuel combustion within the gas generator can be linked to the different roles played by oxygen in the various constituent paths.

Since the reaction mechanism was constructed from separate compilations, verification of the combined scheme against more elementary combustion data was employed to provide a link to the experimental combustion data base. The mechanism was validated against roughly 40 independent sets of experimental data, including ignition delay time and shock tube results, turbulent flow reactor data, and perfectly stirred reactor species profiles.[3] Validation was performed predominantly for fuel-rich mixture conditions at pressures above atmospheric and temperatures representative of those in the gas generator of interest.

Typical Model Comparisons to Data

A sample of the agreement between model predictions and experimental data is given in Figs. 3–8 with the complete results presented in Ref. 3. Good agreement is realized for the specific parent fuel molecules as well as several of the important intermediates in each case. The comparisons of model predictions to experimental data shown in Figs. 3–5 were obtained using the baseline PSR formulation which is free of the modifying fluid physics incorporated into the full gas generator model (PSRVAP).

Typical fuel-rich ethylene oxidation in PSR is shown in Figs. 3a and 3b, which indicates favorable modeling of this important hydrocarbon intermediate to *n*-octane oxidation. The major species ethylene and the intermediates methane, CO and CO_2, match the data[18] very well. Propene, which is also an important intermediate in *n*-octane oxidation, is modeled in Figs. 4a and 4b. Here, important correspondences to the data[19] include propene, ethylene, methane, hydrogen, CO, and CO_2. *n*-Heptane, which is similar to octane as a large alkane in common fuels, is compared to PSR data from Chakir et al.[14] in Figs. 5a and 5b. Both large initial and intermediate species, as well as the important lighter hydrocarbons of ethylene and methane, are in agreement with data.

Good comparisons to ignition delays for the large hydrocarbons *n*-heptane[20] and *n*-octane[13] under a variety of conditions are demonstrated in Figs. 6 and 7. Varying degrees of agreement are realized, with delays predicted too long in a few cases. These ignition delay comparisons are important because they indicate mechanism functionality at high temperatures as well, up to 1650 K. As shown in Fig. 7b, both benzene and toluene ignition delay data[21] at elevated tem-

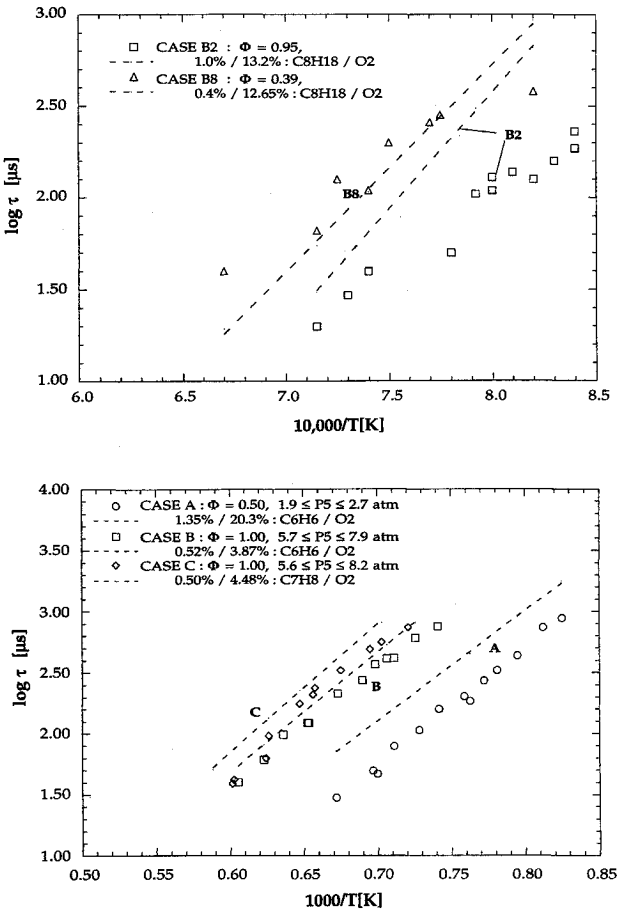

Fig. 7 Ignition delay times for *n*-octane and for aromatics behind reflected shock wave: a) *n*-octane at Φ = 0.95 and 0.35 with data from Burcat et al.[13] and b) benzene at Φ = 0.5, 1.0 and toluene at Φ = 1.0, for various pressures with data from Burcat et al.[21]

peratures and pressures have been modeled successfully with our chemistry model. Better agreement is realized for toluene oxidation than for benzene, a point which we shall address in the gas generator modeling discussion.

Figures 8a and 8b further demonstrate the modelability of the aromatic species toluene and benzene, plus their intermediates. For this test case the important species are all treated well, specifically those oxygenated compounds such as phenol (C_6H_5OH) and benzaldehyde (C_6H_5CHO) that play a crucial role in low temperature ($T < 1700$ K) decomposition.

The importance of these comparisons is to demonstrate that the fuel decompositions are in each case modeled appropriately and that the appearance of important intermediates is predicted.

Experimental Description

The gas generator and chemical reaction model were developed for application to an efflux simulator under experimental investigation. The device is a liquid fueled apparatus burning a mixture of JP-7 and toluene in an oxygen stream. The fuel-oxidizer selection approximates the combustion of a typical solid rocket grain or liquid fueled rocket.[1] Buckley and Corporan have previously documented the device's c^* characteristics over a range of pressures up to 22 atm. More recently, attention has focused on efflux sampling[2] for documentation purposes. Typical experimental results are modeled in this article.

The prototype gas generator is shown schematically in Fig. 9. The device has been run with a JP-7/toluene fuel mixture with representative C/H/O atom balance of $C_{0.363}H_{0.531}O_{0.106}$. This was approximated experimentally by the mixture mole ratio

$$0.122C_{10}H_{21} + 0.346C_7H_8 + 0.532O_2 \qquad (15)$$

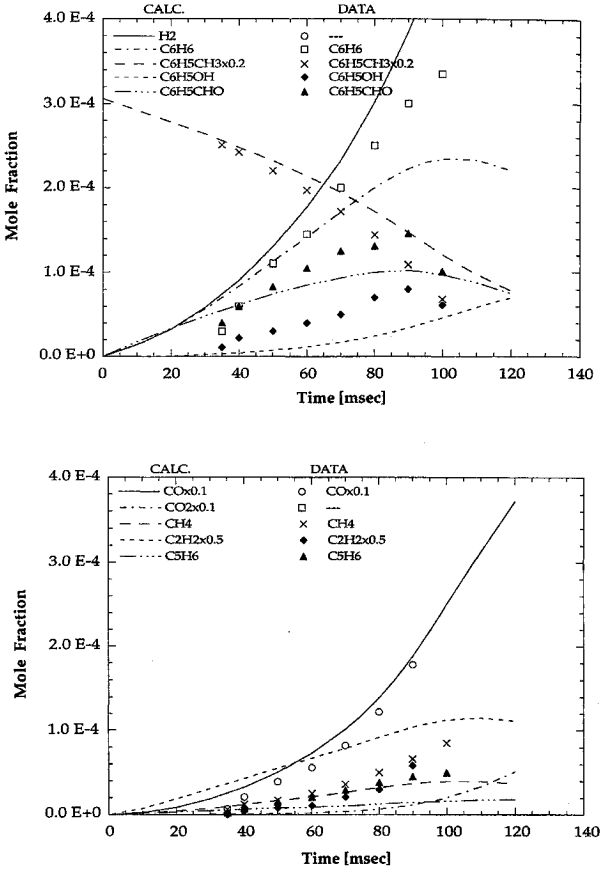

Fig. 8 Toluene oxidation in perfectly stirred reactor at 1 atm, Φ = 0.69, and initial temperature 1188 K: a) major aromatic species and b) selected intermediates and final products. Calculation is compared to data published in Emdee et al.[15]

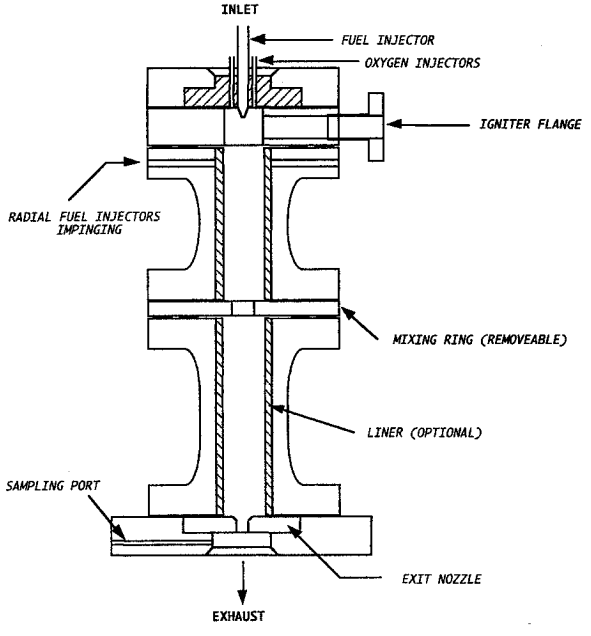

Fig. 9 Experimental gas generator solid fuel efflux simulator.

Since JP-7, with representative formula $C_{10}H_{21}$, is itself a complex mixture of several hydrocarbons (aliphatic and aromatic), we have used the simulated mixture (16) containing *n*-octane and toluene with resulting mole ratios

$$0.127C_8H_{18} + 0.358C_7H_8 + 0.515O_2 \qquad (16)$$

Table 1 Representative experimental operating conditions required for code execution

Variable	Description
P_c	$5.4 \leq P_c \leq 11.9$ atm
$\dot{m}$	$111.0 \leq \dot{m} \leq 150.0$ g/s
V	1573 cm^3 (liner removed)
T_c	$945 \leq T_c \leq 1323$ K

Table 2 Experimental conditions for the test cases in Figs. 10–12

Case no.	1	2	3
MR	0.387	0.346	0.364
P_c, atm	5.44	8.64	11.56
T_c, K	1194	1255	1323
$\dot{m}$, g/s	111.0	111.2	148.0
C_7H_8	0.339	0.347	0.337
JP-7	0.119	0.122	0.119
O_2	0.542	0.531	0.544

Table 3 Comparison of experimental (ept'l.) to model predicted (mod'l.) combustion temperatures (K) and total residence times (tot'l.) to droplet vaporization times (vapr.)[ms]

No.	T, exp'l.	T, mod'l.	τ, tot'l.	τ, vapr.
1	1194	1100	18.6	4.36
2	1255	1147	27.3	3.94
3	1323	1230	25.6	3.56

in place of the experimental one. Similar approximations have been previously employed in combustion modeling.[10]

Several gas sampling experiments have been conducted in a series of separate tests.[2] A commercial five column gas chromatograph equipped with a thermal conductivity detector (TCD) and flame ionization detector (FID) was used to measure the samples taken during the gas generator runs. The five columns and two detectors were needed to correctly separate and quantify the gas samples that covered a wide range of constituents. The high boiling point species were eluted after separation in the columns through the FID system, whereas the lighter species were eluted through the TCD. The gas chromatograph was calibrated with several standard gas mixtures containing the expected efflux species in proportions thought to be representative of those in the gas generator sample.

Samples were withdrawn from the operational gas generator starting 5 s into a run sequence in order to fill the sampling lines. Actual analysis was begun about 12 s into each run after the transient processes reached sufficiently low levels. The hot efflux samples were withdrawn and subsequently quenched by standard nozzle expansion techniques to preclude further reaction in the sampling lines. Sampling lines were maintained at approximately 100°C to avoid condensation of volatile species. Solid particulate was removed in a glass sieve prior to entry into the detectors to avoid contamination. All samples were analyzed and recorded immediately after the run sequence.

The range of operating conditions for this series of tests is listed in Table 1. The measured efflux concentrations were obtained in mole percentages for the detection technique employed. Not all quantities which were measured were identified. The unaccounted efflux in the data represents the sum of the unidentified or uncalibrated peaks in the gas chromatograph readings and can be considered to represent an unknown hydrocarbon mixture. Therefore, the raw numbers listed for those species which were identified represent the true fractions.

Average droplet size estimates for the given injection scheme are in the range of 50 μ, as described in either of Refs. 3 or 4. Results were evaluated in the two previous works for initial

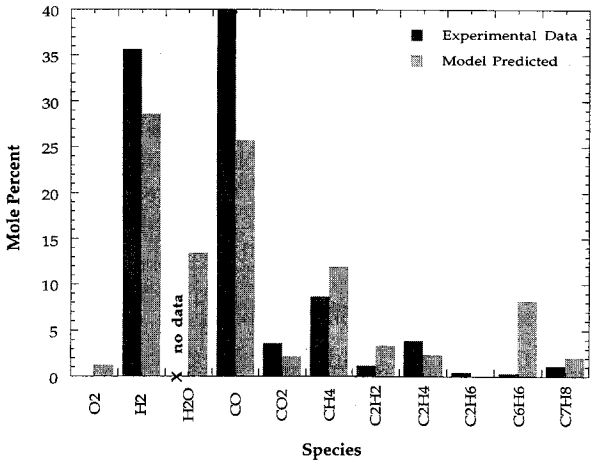

Fig. 10 Comparison of measured and model predicted efflux compositions for case 1 (5.44 atm and 50-μ fuel droplets).

diameters ranging between 50–100 μ as well as gaseous injectants. Only 50-μ results are given here. The reaction zone temperature T_{RXN} was determined for all cases to be 1550 K for this mixture ratio (that which best utilizes the oxygen and maximizes reactor temperature), which is nominally at equivalence ratio 8.95 (MR = 0.362), slightly lower than that given by Eq. (16).

Results and Discussion

The full gas generator model with droplet vaporization considerations and the two-temperature approach was used to model three experimental data cases. The modeled data span the range of pressures covered in the experiments. Comparisons of model-predicted efflux compositions to the experimental data are given in Figs. 10–12a for the cases detailed in Table 2. The results as plotted here exclude the soot contribution which was predicted by the model so that comparison of gas phase species alone could be made to the data. No quantitative data on the amount of sooting was available although sooting does occur. In addition to species data, temperature and residence time comparisons are given in Table 3.

An examination of the efflux composition results indicates several important trends and correspondences to the experimental data. As far as the inlet reactants are concerned, little remaining aliphatic residual and almost complete oxidizer utilization are predicted, both in agreement with experimental data. A considerable amount of the large aromatic toluene is seen to remain unreacted or partially reacted in the form of benzene.

Somewhat higher levels of aromatic are predicted to remain in the efflux than the data support. These findings support earlier findings[3] that aromatic decomposition is severely limited in the low temperature, oxygen-lean gas generator environment. The apparent difficulty with benzene predictions may be related to our simplified equivalent mixture formulation that somewhat overemphasizes the aromatic constituency.

Important stable intermediate species that are in useful form for further combustion include H_2, CH_4, C_2H_2, C_2H_4, and C_2H_6. In general, the levels of these species predicted by the model agree well with experimental data. Ethane levels were generally predicted to be lower than those measured. Ethane's presence under these high-temperature gas generator conditions is not supported by kinetic principals unless a direct production route exists from some higher hydrocarbon source. Such a route is not evident within our chemical mechanism. In any case, ethane is a minor product and we predict this to be the case.

Equilibrium predictions conducted in Ref. 3 indicate that, of the fuels listed above, only hydrogen and methane are present in the gas generator exhaust when combustion proceeds to equilibrium. The equilibrium predictions for case 3

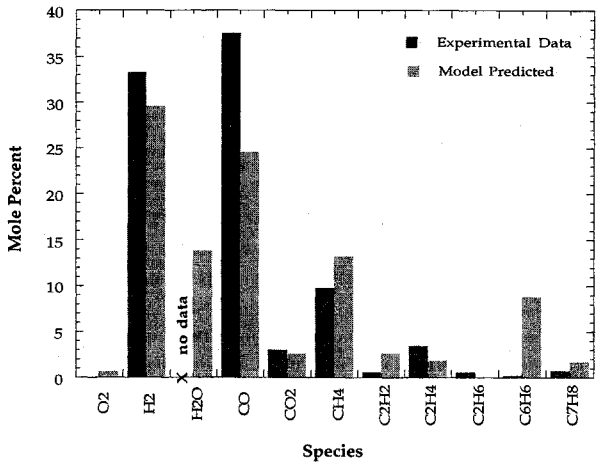

Fig. 11 Comparison of measured and model predicted efflux compositions for case 2 (8.64 atm and 50-μ fuel droplets).

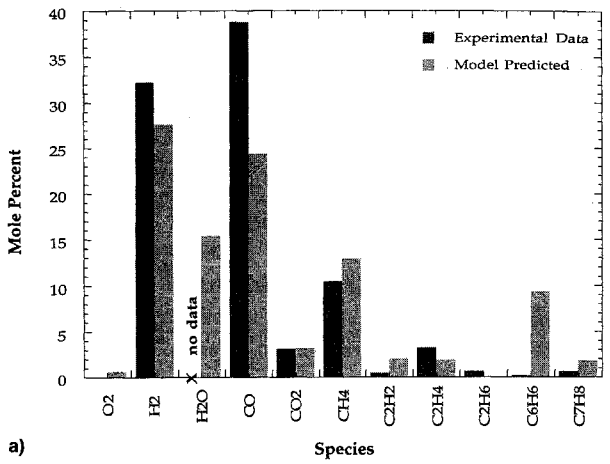

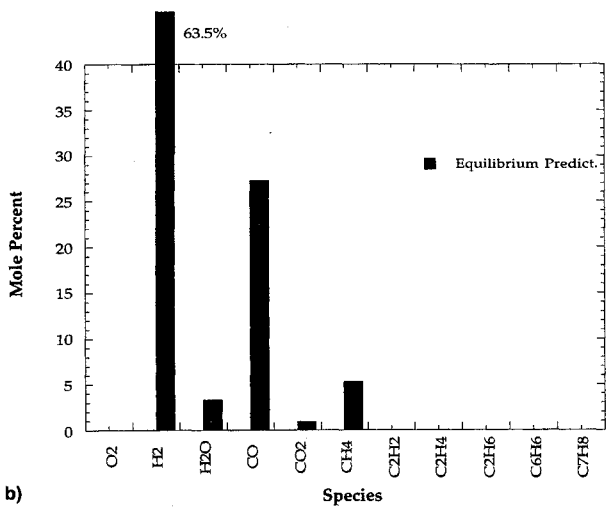

Fig. 12 a) Comparison of measured and model predicted efflux compositions for case 3 (11.6 atm and 50-μ fuel droplets) and b) equilibrium predicted efflux compositions for case 3, indicating no substantial hydrocarbons larger than methane in size. These results are representative for cases 1 and 2 as well.

are included in Fig. 12b, and indicate the large deviation from both measured and nonequilibrium modeled results. The observed presence of hydrocarbon fuels and intermediates such as acetylene, ethylene, and benzene in the experimental efflux is one of several measures indicating operation far from equilibrium.

Product species, such as CO, CO_2, and H_2O are predictable to differing degrees of accuracy. Levels of carbon monoxide are underpredicted by the model in all three cases. The apparent discrepancy is tied to H_2O levels since these two are the only prominent oxygen-containing species in the efflux. Unfortunately, data on H_2O is unavailable leaving this discrepancy unresolved. Large quantities of CO in the exhaust are supported by equilibrium and stoichiometry arguments; however, for this high equivalence ratio, the large CO levels would tend to indicate substantial conversion to final products, which does not seem to be the case based on the content of unburned hydrocarbon. Predicted CO_2 levels agree well with the data, considering the difficulty with CO predictions.

From the standpoint of further efflux combustibility, the smaller hydrocarbons such as methane, acetylene, and carbon monoxide as well as hydrogen are well positioned for secondary combustion in our high-speed propulsion application. The high content of predicted aromatic such as benzene is less desirable for such applications. Benzene could pose problems concerning sooting at these high pressures and low temperatures, especially if long delay times are encountered prior to combustion. Benzene is also a larger, more stable hydrocarbon that is more difficult to combust than the corresponding chain compounds in the gas generator efflux. Product distributions as reported here are consistent with the results of other fuel-rich studies[6] and relevant solid fuel exhaust properties.[17]

Table 3 shows a comparison of predicted to experimental temperatures indicating generally good agreement. For the three cases evaluated in this article, model predictions tended to be low; reverse trends were predicted for several of the lower temperature test cases compared in Ref. 3. Also shown in Table 3 are predicted total residence times and fuel vaporization times. Total residence times agree well with a design point range of 20–30 ms. Vaporization times are relatively short compared to the total residence times supporting the criterion for our droplet vaporization modification to the PSR physics.

Considerable sooting was predicted for these three test conditions with levels approaching 25% in some cases. Noticeable sooting was observed in all experiments, but levels were never quantified (indirect evidence points to soot levels on the order of 10–15%). Equilibrium predicts up to 45% solid carbon in the exhaust. Although the nonequilibrium results are far below this limit, it is believed that sooting is still somewhat overpredicted by the present mechanism. The kinetic processes considered here have been taken from the gas generator work of Nickerson et al.[10] This mechanism has been shown to predict sooting trends in RP-1 fuel-rich gas generators, thus we have some confidence in the proposed soot initiating steps. The present fuel mixture formulation is quite heavily aromatic however (70% of liquid). Soot is undesirable from the application viewpoint because of carbon deposit concerns or loss of usable carbon, therefore, anything which can be done to suppress sooting is of great importance. The sooting processes in gas generators are not thoroughly understood and a comprehensive, validated scheme for their description is not yet available.

The gas generator model predicts a flame zone to occur in the injection region of the device. Neither sustainable combustion nor observed product distributions are supported by the notion of a uniform reactor temperature between exhaust and injection region. Modeling predictions[3,4] and several preliminary temperature probing investigations[2] have identified the existence of the hot reaction zone near the injectors where high temperatures are prevalent. These higher temperatures result in accelerated chemical reaction and vaporization, processes which we have modeled with our two-temperature approach. Our modeling studies have shown that the overall product distributions are dictated by the extent of reac-

tion which can be attained in this high-temperature region. We therefore conclude that combustion of the fuel-rich mixture is kinetically dominated and secondarily vaporization limited.

In summary, the model PSRVAP incorporates vaporization effects within the limitations imposed by a perfectly stirred reactor idealization and allows adjustment of droplet lifetimes to yield acceptable trends in terms of reaction inhibition due to finite fuel vaporization rates. To model the combustion process in the main reaction zone, the two-temperature model is used to represent the observed zonal characteristics of the gas generator injector region. A temperature determined to be consistent with the actual combustion of injected liquid fuel droplets is used to drive the kinetics, effectively decoupling the bulk fluid dynamic and local chemical processes.

Conclusions

A nonequilibrium combustion model has been developed and evaluated here against experimental data from a fuel-rich hydrocarbon gas generator. The model uses the perfectly stirred reactor formulation, which assumes fully mixed gaseous species and uniform temperature, to describe the gas-phase fluid dynamics. Special considerations are given to the injector region's flame zone. A simplified approach to describing the multidimensional injection, mixing, and combustion phenomenon has been employed here. This procedure is taken in order to isolate the kinetically limited chemical processes. The operational aspect of fuel-rich devices which had not been addressed until now is the role that finite rate chemistry has on overall operability.

The most important aspects of our study include the following:

1) A complex hydrocarbon mechanism capable of describing kerosene type fuel mixtures has been developed. The mechanism describes the oxidation and pyrolysis of species up to C8-alkanes in size, plus the aromatics toluene and benzene, and includes a simplified carbon formation description applicable to fuel-rich gas generators.

2) We have modeled a JP-7/toluene fuel mix through a simulated mixture of *n*-octane and toluene. Such an approach has avoided use of semiglobal fuel decomposition steps for JP-7. Using the fundamental approach should allow extension to modeling other complex hydrocarbon fuel mixtures.

The full gas generator combustion model has been successfully applied to describe measured exhaust compositions and combustion temperatures of a fuel-rich hydrocarbon gas generator/preburner. Several key conclusions can be drawn concerning the model application to the particular configuration of interest.

1) Model predictions are able to describe principle experimental efflux compositions. A significant content of aromatic hydrocarbon fuel as well as combustible stable intermediates is predicted. The hydrocarbon intermediates include hydrogen, methane, acetylene, and ethylene (or ethane), and benzene.

2) The two-temperature approach undertaken has been shown to describe the fundamental physical/chemical processes during steady-state operation.

3) The kinetics in the reaction zone dominate the overall observed extent of reaction. The injector configuration flow properties and flame-holding temperature in the gas-liquid region determine the kinetic behavior.

4) The temperature and oxidation characteristics of the reaction zone have the most critical influence on the resulting combustion. When the temperature in the reaction zone remains too low, combustion may no longer be sustainable (flameout), whereas excessive temperatures in this zone will convert much of the usable hydrocarbon into soot precursors.

5) A highly combustible efflux is produced. This flow contains many low molecular weight hydrocarbon fuels. However, the mixture formulation employed here produces significant amounts of unburned aromatic fuels as well, which in the gas generator act principally as diluent. Furthermore, this aromatic decomposes very sluggishly into lighter species. Modeling studies showed long residence times encourage the formation of soot.[3]

The capability of the gas generator model formulation PSRVAP is displayed with sufficient accuracy to indicate that the present system may be used to evaluate fuel-rich gas generator combustion characteristics for design purposes, predict performance trend variations with other flow properties of interest, and to provide the initial point for ramburner combustion studies.

Acknowledgments

The authors R. O. F., J. M. K., and W. C. S. are grateful for the support of the Aeropropulsion and Power Directorate of Wright-Patterson Air Force Base, Dayton, Ohio, during the course of the present investigation. This work was conducted in part under Contract F33615-89-2912.

References

[1]Buckley, P. L., "Progress in the Development of a Hydrocarbon Fueled Gas Generator for Ramrocket Propulsion Research," Australian Aeronautical Conf., Melbourne, Australia, 1989.

[2]Corporan, E., "Efflux Analysis of a Ducted Rocket Gas Generator Simulator," JANNAF Propulsion Meeting, Oct. 1992.

[3]Foelsche, R. O., "A Non-Equilibrium Systems Approach to Modeling Fuel Rich Gas Generator Exhaust Properties," M.S. Thesis, Aeronautical and Astronautical Engineering, Univ. of Illinois, Urbana, IL, 1993.

[4]Keen, J. M., "Computational Modeling of Kinetic Processes in a Gas Generator Experiment," M.S. Thesis, Aeronautical and Astronautical Engineering, Univ. of Illinois, Urbana, IL, 1993.

[5]Desaulty, M., and Chauveau, Y., "Combustor Modeling by Assembly of Well-Stirred Reactors," *Compilation of Symposium Papers, 6th International Symposium on Air Breathing Engines* (Paris, France), AIAA, New York, 1983, pp. 50–55 (AIAA Paper 83-7006).

[6]Heubner, A. W., "High Pressure LOX/Hydrocarbon Preburner Injector Investigation," AIAA Paper 82-1152, June 1982.

[7]Lawver, B. R., "Test Verification of LOX/RP-1 High-Pressure Fuel/Oxidizer-Rich Preburner Designs," AIAA Paper 82-1153, June 1982.

[8]Glarborg, P., Kee, R. J., Grcar, J. F., and Miller, J. A., "PSR: A FORTRAN Program for Modeling Well-Stirred Reactors," Sandia National Labs. Rept. SAND86-8209, Albuquerque, NM, Dec. 1986.

[9]Spalding, D. B., "The Combustion of Liquid Fuels," *Fourth Symposium (International) on Combustion*, The Combustion Inst., Pittsburgh, PA, 1953, pp. 847–864.

[10]Nickerson, G. R., and Johnson, C. W., "A Soot Prediction Model for the TDK Computer Program," AIAA Paper 92-3391, July 1992.

[11]Foelsche, R. O., Keen, J. M., and Solomon, W. C., "A Chemical Kinetic Reaction Mechanism and Thermodynamic Database for Fuel Rich Hydrocarbon Combustion Modeling," Univ. of Illinois, Univ. of Illinois Library Rept. UILU 93-0513, Urbana, IL, Aug. 1993.

[12]Warnatz, J., "Chemistry of High Temperature Combustion of Alkanes up to Octane," *Twentieth Symposium (International) on Combustion*, The Combustion Inst., Pittsburgh, PA, 1984, pp. 845–856.

[13]Burcat, A., Pitz, W. J., and Westbrook, C. K., "Shock Tube Ignition of Octanes," Western States Section Meeting of the Combustion Inst., Lawrence Livermore National Lab. Preprint UCRL-102001, Livermore, CA, Oct. 1989.

[14]Chakir, A., Bellimam, M., Boettner, J. C., and Cathonnet, M., "Kinetic Study of *n*-Heptane Oxidation," *International Journal of Chemical Kinetics*, Vol. 24, No. 4, 1992, pp. 385–410.

[15]Emdee, J. L., Brezinsky, K., and Glassman, I., "A Kinetics Model for the Oxidation of Toluene near 1200 K," *Journal of Physical Chemistry*, Vol. 96, No. 5, 1992, pp. 2151–2161.

[16]Brezinsky, K., "The High-Temperature Oxidation of Aromatic Hydrocarbons," *Progresses in Energy and Combustion Science*, Vol. 12, 1986, pp. 1–24.

[17]Zaccardi, V. A., and McGregor, W. K., "Investigation of the Effluent of a Solid Propellant Gas Generator," Arnold Engineering Development Center Rept. AEDC-TR-83-11, Arnold Air Force Station, TN, April 1983.

[18]Dagaut, P., Cathonnet, M., Boettner, J. C., and Gaillard, F., "Kinetic Modeling of Ethylene Oxidation," *Combustion and Flame*, Vol. 71, No. 3, 1988, pp. 295–312.

[19]Dagaut, P., Cathonnet, M., and Boettner, J. C., "Experimental Study and Kinetic Modeling of Propene Oxidation in a Jet Stirred Flow Reactor," *Journal of Physical Chemistry*, Vol. 92, No. 3, 1988, pp. 661–671.

[20]Burcat, A., "Shock Initiated Ignition in *n*-Heptane-Oxygen-Argon Mixtures," *Proceedings of the 13th International Symposium of Shock Tubes and Waves*, edited by C. E. Treanor and J. G. Hall, State Univ. of New York Press, New York, 1981, pp. 826–833.

[21]Burcat, A., Snyder, C., and Brabbs, T., "Ignition Delay Times of Benzene and Toluene with Oxygen in Argon Mixtures," NASA Lewis Research Center, NASA TM 87312, Cleveland, OH, May 1986.